

# Inkjet-Printed Patterned Quantum Dots Film for High-Efficiency Displays

Pengsen Lin, Xiaoxiao Ji, Luqiao Yin , and Jianhua Zhang 

**Abstract**—Due to the effect of solution kinetics and crystallization kinetics of quantum dot (QD) during inkjet printing, the inkjet printing technique is prone to form coffee-ring patterns and in-homogenous films. Pioneering efforts are usually limited to mixed solvent or additive inks, in this paper, we investigated polymer QD films with good uniformity obtained by inkjet printing, in order to control the uniformity of quantum dot films in pixels, the mechanism of action of wettability science on inkjet printing was considered through the action of nitrous oxide (N<sub>2</sub>O) on the surfaces of substrates and banks. In the absence of N<sub>2</sub>O treatment, the inkjet-printed QD droplets would pile up and adhere to the bank walls due to capillary forces before the pinning process. With the N<sub>2</sub>O surface treatment, the contact angle of the QD ink on the substrate was increased from 16° to 62°. The wettability of the QDs between the substrate and the bank was reduced, and the side build-up phenomenon was significantly reduced. By changing the thickness of the QD film from 4.5 μm to 15 μm, the color coordinates of the spectrum were changed from (0.2320, 0.1556) to (0.1480, 0.6933).

**Index Terms**—Quantum dots, inkjet printing, surface treatment, color coordinates.

## I. INTRODUCTION

MICRO light-emitting diodes (micro-LEDs) refers to a high-density tiny-sized LED array integrated on a chip, and the pixel size is generally less than 100 μm, GaN-based micro-LEDs have broad application prospects in display, visible light communication and other fields [1]. However, despite such excellent performance, micro-LEDs displays still face many difficulties in commercial mass production. The two main technical problems of this technology are the mass transfer of LED chips [2] and the production of full-color displays [3]. To realize the color conversion of micro-LEDs, quantum dot light-emitting diodes (QD-LEDs) with patterned QD films are chosen as color conversion layers (CCLs) [4], [5], [6]. This produces green light

Manuscript received 27 September 2022; revised 29 October 2022; accepted 9 November 2022. Date of publication 14 November 2022; date of current version 21 November 2022. This work was supported in part by the Science and Technology Commission of Shanghai Municipality Program under Grants 20010500100, 21511101302, and 19142203600 and in part by the National Nature Science Foundation of China under Grants 51725505 and 51605272. (Corresponding author: Luqiao Yin.)

Pengsen Lin is with the School of Materials Science and Engineering, Shanghai 20444, China (e-mail: linpengsen@shu.edu.cn).

Xiaoxiao Ji is with the School of Mechatronics and Automation, Shanghai 200072, China (e-mail: jixx@shu.edu.cn).

Luqiao Yin and Jianhua Zhang are with the Key Laboratory of Advanced Display and System Applications, Ministry of Education, Shanghai University, Shanghai 200072, China (e-mail: lqyin@shu.edu.cn; jhzhang@oa.shu.edu.cn).

Digital Object Identifier 10.1109/JPHOT.2022.3221777

by pumping QDs through a short-wavelength electroluminescent chip, without the need for a mass transfer process [7]. Because QD-LEDs use QD films as color-conversion layers, they have lower light loss than white Organic Light Emitting Diode (OLED) [8], [9]. This approach is also considered to be one of the most likely solutions for next-generation display technologies (including micro-LEDs), among others [10].

For patterning, the photolithography-etch process is the most established method. However, there are several main technical difficulties in the preparation of QD color photoresist. QDs are easily quenched when encountering water and oxygen, so the requirements for QD materials themselves are very high [11], [12]. The advantage of lithography is to form patterns with fine pitches, but it does not guarantee low material consumption and the fabrication steps are cumbersome [13]. In the vacuum deposition process, the yield of the material from the source to the deposited film is low, compared to photolithography, Inkjet printing is the best candidate for producing large-scale patterned QD films with little material waste, simple process, low cost, highly automated, and maskless patterning.

With the improvement of the resolution in the display field, while meeting the needs of the pixel size, the previously printed pixel units are often larger than 100 microns, and the current mainstream technology should achieve the pixel size below 50 microns. To ensure that the ultraviolet light emitted by the UV LED does not leak, the printed QD color conversion layer film requires a thickness of a few microns. When an ink droplet with a diameter of tens of micrometers lands on the target point, the final morphology of the ink droplet is related to the surface energy of the substrate [14]. On hydrophilic surfaces, it tends to have good wettability, on hydrophobic surfaces, it tends to have poor wettability [15]. Typical drop sizes available with current inkjet printheads range from 10 to 100 μm in diameter (or 0.5 to 500 pl in volume) due to droplet generation limitations. There have been some previous studies investigating the application of various surface treatments to control surface wettability to form homogeneous films. They often applied chemical coatings and physical engineering to make substrates and banks hydrophilic and hydrophobic, and the film thickness that can be achieved below 1 micron, which cannot meet the needs of thick film, and the problem of film thickness non-uniformity occurs [16], [17]. Therefore, it is urgent to develop a new way to meet the uniformity of thick films.

In this paper, we used inkjet printing to develop green matrix patterns. The substrates and banks used were treated with hydrophobic N<sub>2</sub>O, and a uniform QD color conversion layer

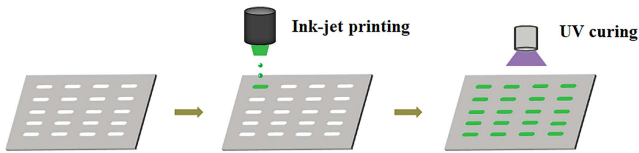


Fig. 1. Process schematic of UV-cured green QD color conversion layer prepared using inkjet printing method.

of more than ten microns was formed on the sample, and the thickness was controlled by inkjet printing instead of the usual Samples treated with hydrophilic substrates and hydrophobic banks.  $N_2O$  plasma surface treatment is a dry process with short treatment time and high efficiency. Improve the surface energy of the material without changing the intrinsic properties of the material. By treating the substrate and dam with different wettability, the effect of photoresist surface wettability on the shape of the printed film was studied. With optimized surface wettability, the light conversion efficiency (LCE) from UV light to green light can be achieved by adjusting the thickness of the QD layer.

## II. EXPERIMENTAL SECTION

The process to prepare the patterned QD film is illustrated in Fig. 1. A bank structure where QD ink is ejected from a piezoelectric nozzle onto a substrate. The ink is confined by the black matrix with an average depth of  $15 \mu\text{m}$  and effectively prevents the diffusion of the QD ink. After printing, it cured by UV light.

Blocking dams are required between pixels, and in order to create a color conversion layer that converts UV light into green light. We compared photoresists with different viscosities, and finally chose 420 cP as the best solution. In order to reduce the optical crosstalk effect in the previous work, a mold with windows and retaining walls was prepared. In addition, the shape and size of the prepared banks were analyzed using an optical microscope (OM; VHX-5000; KEYENCE) and an image analysis program, the bank pattern was made using conventional photolithography, Process (spin coating, pre-bake, UV exposure, post-bake and develop). As shown in Fig. 2(c) and (d). The embankment is  $32.4 \mu\text{m}$  wide,  $32.4 \mu\text{m}$  long and  $15 \mu\text{m}$  high. The bank material is fluoroacrylate monomer and fluoroacrylate oligomer.

The surface treatment of the substrate affects its surface energy and surface roughness, which in turn changes the wettability of the black matrix. To remove surface oil stains, the substrates were sonicated in an acetone solution for 15 minutes. Next, UV ozone surface treatment was performed on the substrate for 20 minutes. After cleaning, the banks were fabricated using conventional photolithography, and then the samples were then surface treated with  $N_2O$  by PECVD method. For contact angle measurements, SL200K (Kino, USA) was used to evaluate the wettability of the black matrix with glass substrate.

The printer model we used was a Dimatix DMP 2831, and it was paired with a DMC-11601 ink cartridge (Fujifilm, Japan)

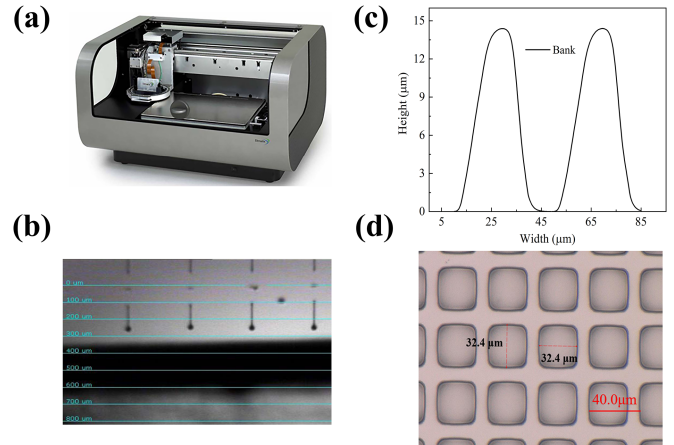


Fig. 2. (a) Image of the DMP 2831 inkjet printer, (b) the picture of droplet falling from the nozzles, (c) the depth between the two embankments measured with a  $\alpha$  step meter, (d) and an optical microscope picture of the bank pattern formed.

for fine print. And by dynamically adjusting the jetting waveform, firing frequency, firing voltage, printing height, substrate temperature and ink cartridge temperature, the smooth jetting conditions for QD inks were successfully found. Viscous ink droplets without trailing fluid or satellite droplets were achieved, ensuring reliable and continuous ink printing. Fig. 2(a) shows a photograph of the DMP 2831 inkjet printer, (b) the image of the QD ink droplet ejected from the nozzle, (c) the depth of the embankment measured in a single step, (d) and optical microscope image of the formed bank pattern. After printing the quantum dots with different layers, we carried out the encapsulation process. For the encapsulation process, a glue dispenser (300DS, Musashi Engineering Inc.) was used to apply a low viscosity UV glue to the edge of the glass cover and cured with UV light for 5 minutes. The entire encapsulation process was performed in a nitrogen ( $N_2$ ) atmosphere glove box.

## III. RESULTS AND DISCUSSION

The photoluminescence (PL) and UV-vis absorption spectra of the QDs are shown in Fig. 3, The emission peak is located at 516 nm and 627 nm, and the full width at half maximum (FWHM) is 31 nm and 28 nm.

Fig. 4 shows the contact angle images of water on the glass substrate and the bank. The screen shows that the water contact angle in the black matrix without surface treatment shows hydrophobic properties, and the value is  $85^\circ$ , and the value decreases after treatment. In addition, water exhibits hydrophilic properties on glass substrates, and its hydrophilicity increases after UV ozone treatment. After treatment with  $N_2O$  hydrophobic molecules, the contact angle increased significantly, as previously reported in the literature [18], [19], [20], [21]. However, the water-to-glass contact angle was  $16^\circ$  without surface treatment and  $85^\circ$  on the shore, and after  $N_2O$  treatment, the glass-to-water contact angle increased from  $16^\circ$  to  $62^\circ$ , the surface energy between the bottom of the cavity and the sidewall of the black

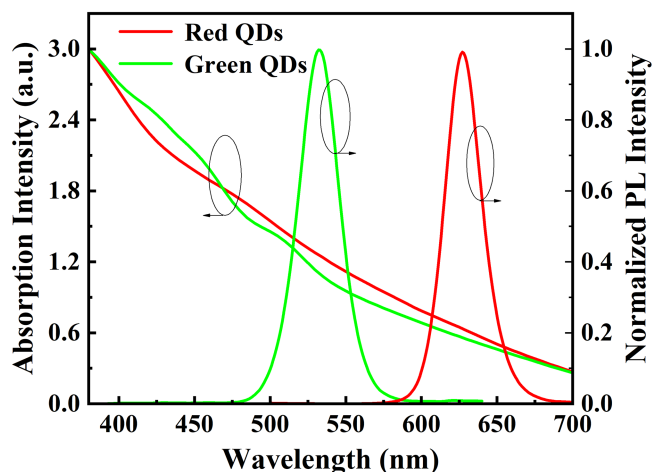


Fig. 3. Absorption and PL spectra of the green/red QDs.

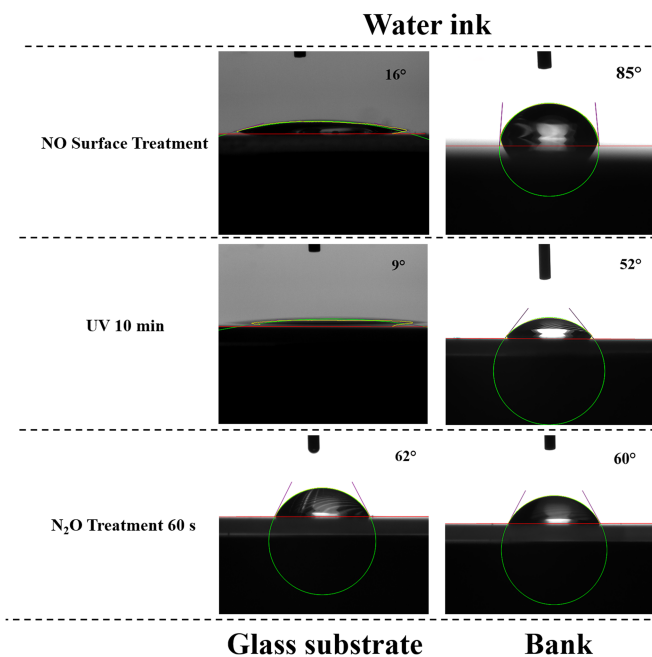


Fig. 4. Image of water contact angle measured on glass substrate and black matrix.

matrix changes, and the green QD ink can be smoothly deposited in the pixel dots surrounded by the black matrix. Due to the difference in wettability, the QD droplets formed by successive stacking with increasing thickness have poor diffusivity and will not be trapped in the bank but accumulate on the bank wall, a flat QD film cannot be formed. It is found that  $N_2O$  can reduce the wettability of QD inks on glass and banks. And it will increase the printing thickness of the QDs and reduce the leakage of UV light.

The film formation process of the droplets is: (i) impingement of the droplet on the substrate, (ii) spreading, (iii) pinning [22], [23], [24]. Here, the characteristic pattern of deposition is attributed to a form of capillary flow, pinning of the contact lines induces outward convective flow as evaporation proceeds,

and the pinning process of droplets is strongly related to the surface energy of the substrate. At the perimeter of the sidewall, the liquid shrinks, but the radius does not decrease because its contact line is fixed. In the previous literature, increasing the wettability of the substrate increases the size of the final formed droplet ejected from the ink port, while decreasing the wettability of the substrate decreases the size of the droplet after falling [18].

In order to confirm the speculation that wettability affects the surface shape and size, a simulation analysis was carried out, in which the size of the substrate surface and black matrix wettability was selected as the main influencing factor of the deposition effect. First, for the substrate without surface treatment, the glass contact angle is  $16^\circ$  and the photoresist contact angle is  $60^\circ$ ; for the  $N_2O$  treated substrate, the glass contact angle is  $38^\circ$  and the photoresist contact angle is  $89^\circ$ . Obviously, when treated, the wettability is reduced, and a weakened capillary phenomenon can be observed, as shown in Fig. 5 below. These simulation results show that the reduction of the surface energy of the substrate has a promoting effect on the formation of a flat and uniform QD film.

Controlling the deposition process is critical for making thin films with high uniformity due to size effects, as shown in Fig. 6(c) and (d), after  $N_2O$  treatment of the substrate for 1 minute, the QD films could be uniformly formed under the microscope, The QD films without surface treatment were mainly distributed at the edge of the pixel. Without surface treatment, the printed QD droplets could not form a uniform film, but spread on the substrate and accumulated heavily on the bank walls, as shown in Fig. 6(a). High surface wettability, the three-phase contact lines of the ink droplets were located on the bank, and the shape of the print was determined by the contact angle. However, for 60 s of  $N_2O$  treatment, the pinning process hardly occurred, as shown in Fig. 6(b). Since the bank space was small, to ensure the printing effect, we used a 1 pl nozzle to control the final morphology and thickness of the QD film in the black matrix pixel unit.

Fig. 7(a) and (b) show the thickness and luminescence images of the inkjet-printed QD layer without any treatment, the step meter showed that the inkjet-printed QD droplets formed QD films on the bank walls, for UV/ozone treated the sample, the thickness of the QD films became smaller because the wettability of both the substrate and the bank was increased, and more UV light was transmitted out, forming a concave in the middle and a convex image around it. When the wetting was reduced by  $N_2O$ . The thickness of the QD film increased and became smoother, and the ability to absorb ultraviolet light became stronger.

The color was patterned by inkjet printing, and the relationship between the color conversion efficiency and the thickness of the QD color conversion layer was discussed, the QD color conversion layer was inkjet printed on the bank patterned substrate with controllable thickness with different numbers of inkjet printing droplets after 60 s  $N_2O$  treatment. Fig. 8 shows the color coordinates of different thicknesses of inkjet-printed green QD color conversion layers. As the number of printed drops increased from 15 to 60 drops, the UV LED intensity decreased significantly and the green light intensity increased significantly.

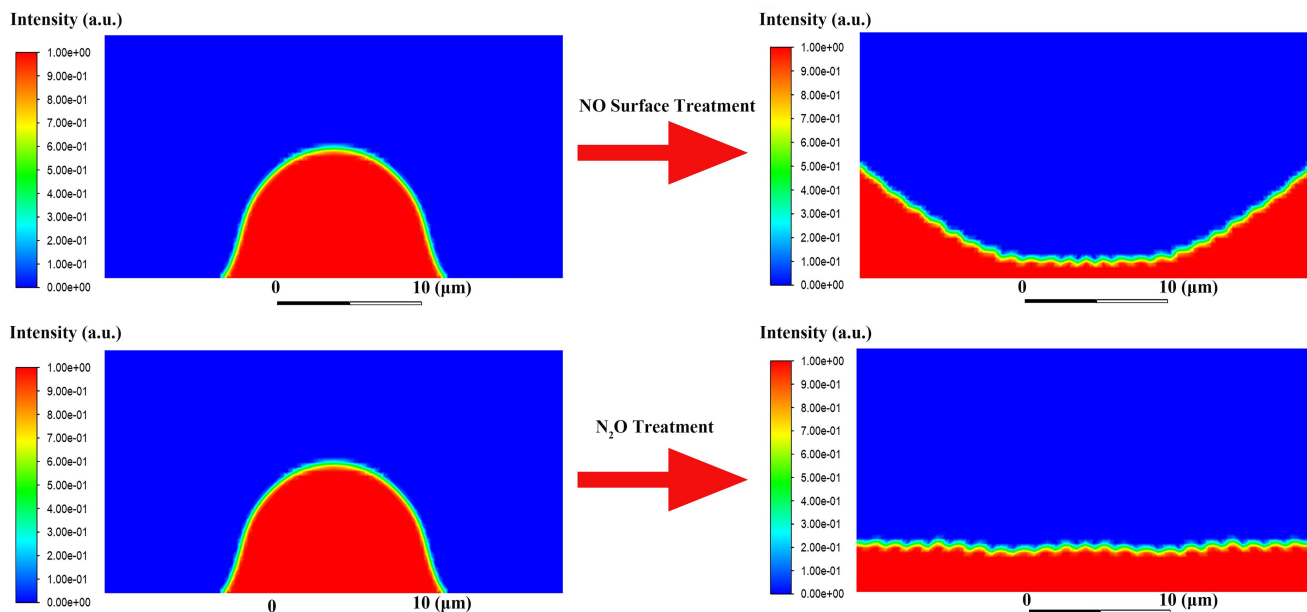


Fig. 5. Droplet deposition simulation. Simulation results of unsurfaced and  $N_2O$  treated models.

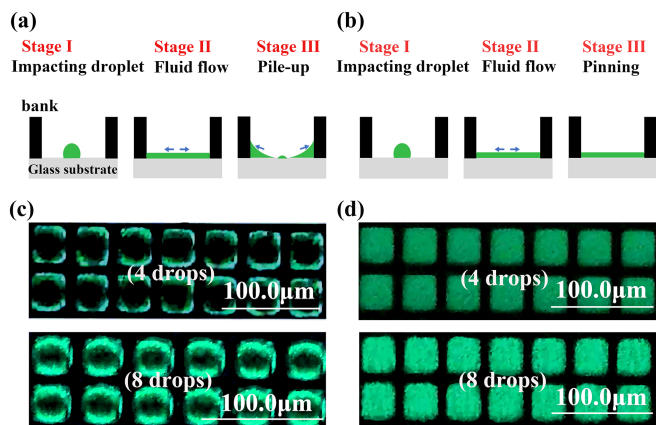


Fig. 6. Illustration of the film-forming drying behavior after droplet fall: (a) Without surface treatment, (b)  $N_2O$  treatment of 60 s. Images of green QD films using a 1 pl nozzle inkjet-printed optical microscope: (c) Without surface treatment (UV exposure), (d)  $N_2O$  treatment of 60 s (UV exposure).

Fig. 9 shows the comparison of the color coordinates under the three conditions, with the best performance after treatment with  $N_2O$ .

To evaluate the conversion properties, patterned QDs were printed on a 700-micron-thick piece of glass. After soft-baking and UV curing the entire layer, the QD layer on the glass was excited by tightly applying UV backlight LEDs to the backside of the glass. UV backlight LED, square, fabricated using the same GaN epilayer. The UV light will continuously penetrate the glass and the QD layer so that the unabsorbed UV light was collected by the light energy meter along with the converted red or green light. Based on the obtained data, the optical output power of the unabsorbed blue light (PB1) and the converted red

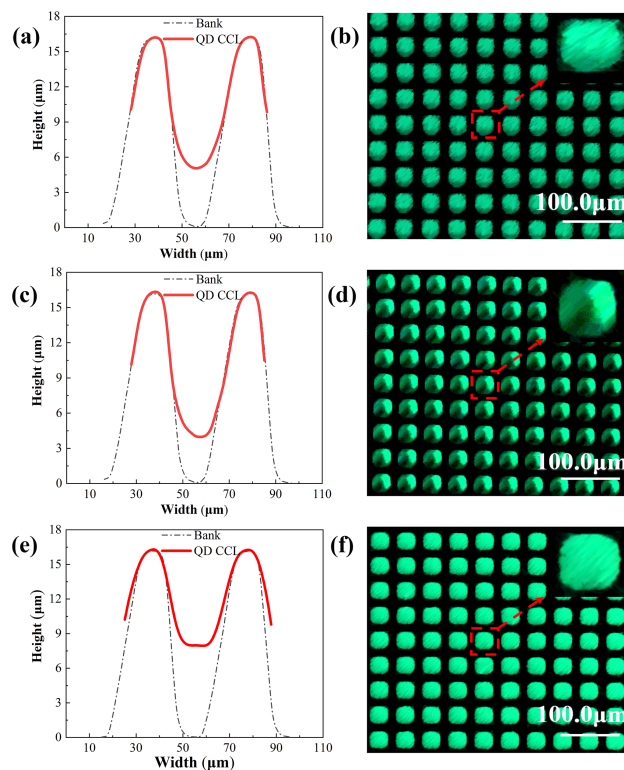


Fig. 7. Thickness distribution and fluorescence images of printed QDs. (a), (b) No surface treatment, (c), (d) After UV treatment for 10 minutes, (e), (f) and  $N_2O$  treatment for 60 s.

light (PR1) or green light (PG1) can be calculated by obtaining the corresponding peak wavelengths. At the same time, in order to calculate the total output blue light power (PB0) through the thin glass and the inkjet printed layer, the same state setting

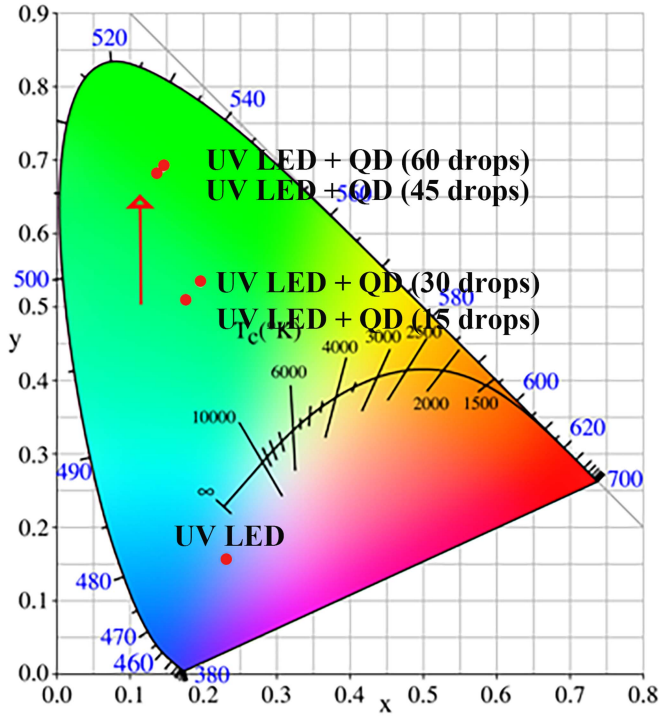


Fig. 8. Thickness of color conversion layers with 15, 30, 45 and 60 drop QDs, and color coordinates of corresponding devices.

was used as a reference by irradiating the bare glass. Therefore, the absorption rate, conversion ratio and power conversion efficiency (PCE) [25] can be defined as follows:

$$\text{Absorption Ratio} = \frac{P_{B0} - P_{B1}}{P_{B0}} \quad (1)$$

$$\text{Conversion Ratio} = \frac{P_{R1}}{P_{B0} - P_{B1}} \text{ or } \frac{P_{G1}}{P_{B0} - P_{B1}} \quad (2)$$

$$\text{Power conversion Efficiency} = \frac{P_{R1}}{P_{B0}} \text{ or } \frac{P_{G1}}{P_{B0}} \quad (3)$$

The switching properties of the green QD layer are shown in Fig. 10. Three samples were measured and compared, with green QD layer thicknesses of 15, 30, 45, and 60 drops, respectively. As shown in Fig. 10(a), in the case of the backlight LED injecting 100 mA current, the absorption rate increases with the increase of green QDs, at high thickness values, the absorption ratio rises more slowly, and as the thickness increases, the maximum absorption ratio will remain unchanged, when the mean free path of the QD film was shorter, its extinction coefficient was larger, and the ability to absorb UV light was stronger. The conversion rate decreased first, then increased and then decreased with the increase of the thickness of the QDs. As the printing progresses, the absorption capacity of the QDs for blue light increases, and the conversion rate tends to decrease. When the printed ink droplet exceeds a certain thickness, due to the overlap between the absorption and emission spectra of the QDs, this may lead to reabsorption, resulting in high conversion losses, resulting in a decrease in the intensity of the converted light.

To better understand the influencing factors of Color Conversion Efficiency (CCE), we defined CCE as the ratio of the green

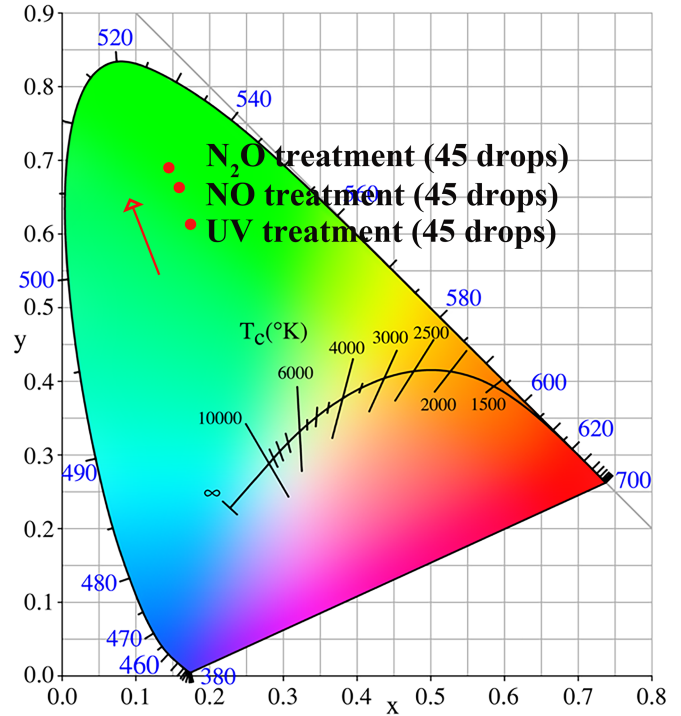


Fig. 9. The thickness of the color conversion layer of 45 drops of QD, and the color coordinates of the corresponding device when untreated, UV treated, N<sub>2</sub>O treated.

light emitted by the QDs to the intensity of the original UV LED (without QDs) [26]. When the current was 100 mA and 15 drops were printed, PG1 was 7.8 mW; PB0 was 97.6 mW; When the current was 100 mA and 30 drops were printed, PG1 was 9.2 mW; PB0 was 97.6 mW; When the current was 100 mA and 45 drops were printed, PG1 was 14.4 mW; PB0 was 97.6 mW; When the current was 100 mA and 60 drops were printed, PG1 was 10.3 mW; PB0 was 97.6 mW; The calculated CCEs of QD color conversion layers with 15 drops, 30 drops, 45 drops and 60 drops were 8.0%, 9.4%, 14.7% and 10.5%, respectively. When the film thickness of the printed QD layer is too thin, the residual UV light cannot be suppressed, so it cannot efficiently convert from UV light to green light. We also found that when the number of printed QD layers exceeds a certain value, the CCE actually decreases. These results may be due to the spectral overlap of the materials themselves. The light from the QDs generated by the color conversion layer competes with the reabsorption by the QDs in the QD film. In order to maintain the advantages of QDs, fluorescence resonance energy transfer (FRET) should be considered, reducing nonradiative recombination and avoiding self-absorption between printed QDs.

Fig. 10(c) depicts the converted green light ( $\lambda = 516 \text{ nm}$ ) along with the unabsorbed UV light ( $\lambda = 365 \text{ nm}$ ) emitted from the green QD layer. For a 60-layer thick green QD layer, the unabsorbed transmitted UV light was still stronger than the converted green light. Therefore, in the actual full-color demonstration, it is essential to apply an extra layer of green CF to block the unabsorbed UV light.

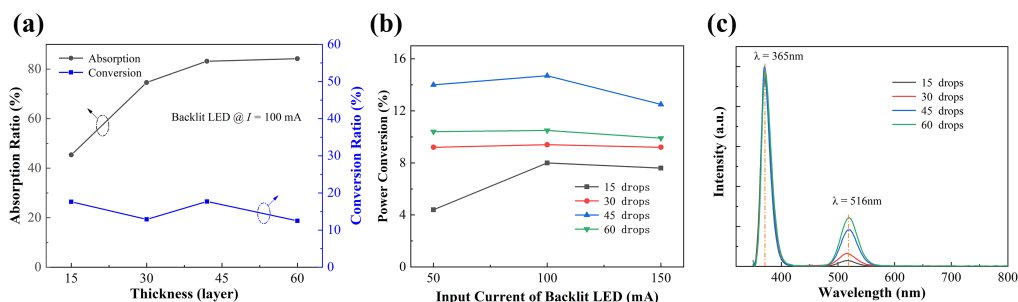


Fig. 10. (a) Absorption/conversion of green QD photo-inkjet-printed layers with different thicknesses when excited by a UV backlight LED with an input current of 100 mA. (b) Power conversion efficiency of green inkjet-printed layers injected into backlight LEDs at different currents. (c) Spectra of unabsorbed UV light and converted green light from green inkjet-printed QD layers with different drops when excited by a UV backlight LED with an input current of 10 mA.

#### IV. CONCLUSION

In this study, in order to make the QD pixels exhibit uniform morphology, we surface-treated the substrate and the dykes. Through the measurement of hydrophobicity and hydrophilicity, the results showed that the contact angle between glass and water was  $16^\circ$  without any treatment, and the contact angle was reduced to  $9^\circ$  after UV treatment for 10 minutes. However, after 60 seconds of  $N_2O$  treatment, the contact angle between glass and water increased to  $62^\circ$ . Furthermore, the QD films were clearly attached to the bank walls before surface treatment, but disappeared after  $N_2O$  treatment. Each pixel exhibits uniform photoluminescence, and the thickness of the thin film within the bank can be evaluated by the number of layers of printed QDs. By changing the thickness of the QD film from  $4.5 \mu\text{m}$  to  $15 \mu\text{m}$ , the CIE chromaticity coordinates of the spectrum changed from (0.2320, 0.1556) to (0.1768, 0.5110), (0.1959, 0.5339), (0.1438, 0.6899) for UV LED and (0.1480, 0.6933), changing from near ultraviolet to near pure green. In addition, printing 45 drops of QDs, we found the largest PCE, which provides some references for the recent mass production of micro-LED full-color micro displays.

#### REFERENCES

- [1] S. Hang et al., "A review on the low external quantum efficiency and the remedies for GaN-based micro-LEDs," *J. Phys. D: Appl. Phys.*, vol. 54, no. 15, Jan. 2021, Art. no. 153002.
- [2] A. Paranjpe, J. Montgomery, S. M. Lee, and C. Morath, "45-2: Invited paper: Micro-LED displays: Key manufacturing challenges and solutions," *SID Symp. Dig. Tech. Papers*, vol. 49, no. 1, pp. 597–600, May 2018.
- [3] Y. Huang, G. Tan, F. Gou, M.-C. Li, S.-L. Lee, and S.-T. Wu, "Prospects and challenges of mini-LED and micro-LED displays," *J. Soc. Inf. Display*, vol. 27, no. 7, pp. 387–401, Mar. 2019.
- [4] E. Chen et al., "Asymmetric quantum-dot pixelation for color-converted white balance," *ACS Photon.*, vol. 8, no. 7, pp. 2158–2165, Jun. 2021.
- [5] Y. Chen et al., "Quantum-dot array with a random rough interface encapsulated by atomic layer deposition," *Opt. Lett.*, vol. 47, no. 1, pp. 166–169, Jan. 2022.
- [6] C. Wang et al., "Full-visible-spectrum perovskite quantum dots by anion exchange resin assisted synthesis," *Nanophotonics-Berlin*, vol. 11, no. 7, pp. 1355–1366, Feb. 2022.
- [7] X. Yang et al., "An overview on the principle of inkjet printing technique and its application in micro-display for augmented/virtual realities," *Opto-Electron. Adv.*, vol. 5, no. 6, Aug. 2022, Art. no. 210123.
- [8] H. V. Demir, S. Nizamoglu, T. Erdem, E. Mutlugun, N. Gaponik, and A. Eychmüller, "Quantum dot integrated LEDs using photonic and excitonic color conversion," *Nano Today*, vol. 6, no. 6, pp. 632–647, Dec. 2011.
- [9] E. Jang, S. Jun, H. Jang, J. Lim, B. Kim, and Y. Kim, "White-light-emitting diodes with quantum dot color converters for display backlights," *Adv. Mater.*, vol. 22, no. 28, pp. 3076–3080, Jul. 2010.
- [10] M. Duan et al., "Inkjet-printed micrometer-thick patterned perovskite quantum dot films for efficient blue-to-green photoconversion," *Adv. Mater. Technol.*, vol. 4, no. 12, Nov. 2019, Art. no. 1900779.
- [11] S. C. Huang, C. W. Yeh, G. H. Chen, M. C. Liu, and H. S. Chen, "Investigation of luminescence enhancement and decay of QD-LEDs: Interface reactions between QDs and atmospheres," *ACS Appl. Mater. Interfaces*, vol. 11, no. 2, pp. 2516–2525, Jan. 2019.
- [12] C.-W. Yeh, G.-H. Chen, S.-J. Ho, and H.-S. Chen, "Inhibiting the surface oxidation of low-cadmium-content ZnS: (Cd, Se) quantum dots for enhancing application reliability," *ACS Appl. Nano Mater.*, vol. 2, no. 8, pp. 5290–5301, Jan. 2019.
- [13] J. Yang, J. Yoo, W. S. Yu, and M. K. Choi, "Polymer-assisted high-resolution printing techniques for colloidal quantum dots," *Macromol. Res.*, vol. 29, no. 6, pp. 391–401, Jun. 2021.
- [14] D. Y. Kim, Y. J. Han, J. Choi, C. Sakong, B.-K. Ju, and K. H. Cho, "Inkjet printed quantum dot film formed by controlling surface wettability for blue-to-green color conversion," *Org. Electron.*, vol. 84, Sep. 2020, Art. no. 105814.
- [15] R. J. Good, "Contact angle, wetting, and adhesion: A critical review," *J. Adhesion Sci. Technol.*, vol. 6, no. 12, pp. 1269–1302, Jan. 1992.
- [16] H. Li, A. Li, Z. Zhao, M. Li, and Y. Song, "Heterogeneous wettability surfaces: Principle, construction, and applications," *Small Struct.*, vol. 1, no. 2, Nov. 2020, Art. no. 2000028.
- [17] H. Y. Park, B. J. Kang, D. Lee, and J. H. Oh, "Control of surface wettability for inkjet printing by combining hydrophobic coating and plasma treatment," *Thin Solid Films*, vol. 546, pp. 162–166, Nov. 2013.
- [18] Y. I. Lee et al., "Effect of UV/ozone treatment on interactions between ink-jet printed Cu patterns and polyimide substrates," *Thin Solid Films*, vol. 519, no. 20, pp. 6853–6857, Aug. 2011.
- [19] P. Q. M. Nguyen, L.-P. Yeo, B.-K. Lok, and Y.-C. Lam, "Patterned surface with controllable wettability for inkjet printing of flexible printed electronics," *ACS Appl. Mater. Interfaces*, vol. 6, no. 6, pp. 4011–4016, Mar. 2014.
- [20] A. Pietrikova et al., "Surface analysis of polymeric substrates used for inkjet printing technology," *Circuit World*, vol. 42, no. 1, pp. 9–16, Feb. 2016.
- [21] A. K. Thokchom, Q. Zhou, D.-J. Kim, D. Ha, and T. Kim, "Characterizing self-assembly and deposition behavior of nanoparticles in inkjet-printed evaporating droplets," *Sens. Actuators, B Chem.*, vol. 252, pp. 1063–1070, Nov. 2017.
- [22] R. D. Deegan, O. Bakajin, T. F. Dupont, G. Huber, S. R. Nagel, and T. A. Witten, "Capillary flow as the cause of ring stains from dried liquid drops," *Nature*, vol. 389, no. 6653, pp. 827–829, Oct. 1997.
- [23] M. Kaneda, K. Hyakuta, Y. Takao, H. Ishizuka, and J. Fukai, "Internal flow in polymer solution droplets deposited on a lyophobic surface during a receding process," *Langmuir*, vol. 24, no. 16, pp. 9102–9109, Aug. 2008.
- [24] J. Lim, W. Lee, D. Kwak, and K. Cho, "Evaporation-induced self-organization of inkjet-printed organic semiconductors on surface-modified dielectrics for high-performance organic transistors," *Langmuir*, vol. 25, no. 9, pp. 5404–5410, May 2009.
- [25] X. Zhang, L. Qi, W. C. Chong, P. Li, C. W. Tang, and K. M. Lau, "Active matrix monolithic micro-LED full-color micro-display," *J. Soc. Inf. Display*, vol. 29, no. 1, pp. 47–56, Aug. 2020.
- [26] V. I. Klimov, "Nanocrystal-based light-emitting diodes utilizing high-efficiency nonradiative energy transfer for color conversion," *Nano Lett.*, vol. 6, no. 7, pp. 1396–1400, Jul. 2006.